Systematic screening of DMOF-1 with NH_2, NO_2, Br and azobenzene functionalities for elucidation of carbon dioxide and nitrogen separation properties

Mingrou Xie[a,‡], Nicholaus Prasetya[a,‡] and Bradley P. Ladewig[a,b,*]

[a]Barrer Centre, Department of Chemical Engineering, Imperial College London, Exhibition Road, London SW7 2AZ, United Kingdom

[b]Institute for Micro Process Engineering (IMVT), Karlsruhe Institute of Technology, Hermann-von-Helmholtz-Platz 1, 76344 Eggenstein-Leopoldshafen, Germany

[‡]Equal contribution

[*]Corresponding author: bradley.ladewig@kit.edu

Abstract

In this study, dabco MOF-1 (DMOF-1) with four different functional groups (NH_2, NO_2, Br and azobenzene) has been successfully synthesized through systematic control of the synthesis conditions. The functionalised DMOF-1 is characterized using various analytical techniques including PXRD, TGA and N_2 sorption. The effect of the various functional groups on the performance of the MOFs for post-combustion CO_2 capture is evaluated. DMOF-1s with polar functional groups are found to have better affinity with CO_2 compared with the parent framework as indicated by higher CO_2 heat of adsorption. However, imparting steric hindrance to the framework as in Azo-DMOF-1 enhances CO_2/N_2 selectivity, potentially as a result of lower N_2 affinity for the framework.

Keywords: metal organic framework, DMOF-1, CO_2 capture and separation

Since its first report in 2004 [1], Dabco MOF-1 (DMOF-1) has been widely investigated, particularly because it has a flexible framework [2, 3]. Other investigations have also shown the promising application of this material for gas storage [4-6]. In this study, we then aim to further investigate the applicability of this material for post-combustion CO_2 separation by functionalizing the parent framework with various functional groups. By changing the synthesis

mixture of DMOF-1, various functionalized DMOF-1s could then be successfully synthesized and the molar ratio between the functionalized ligands and the dabco could be maintained at around 2:1 as also found in DMOF-1 as their parent framework (Figure S2-S6). As can be seen in Figure 1 both NH_2-DMOF-1 and Azo-DMOF-1 crystallized in a rod-shape form while the DMOF-1, Br-DMOF-1 and NO_2-DMOF-1 crystallized in a cubical form.

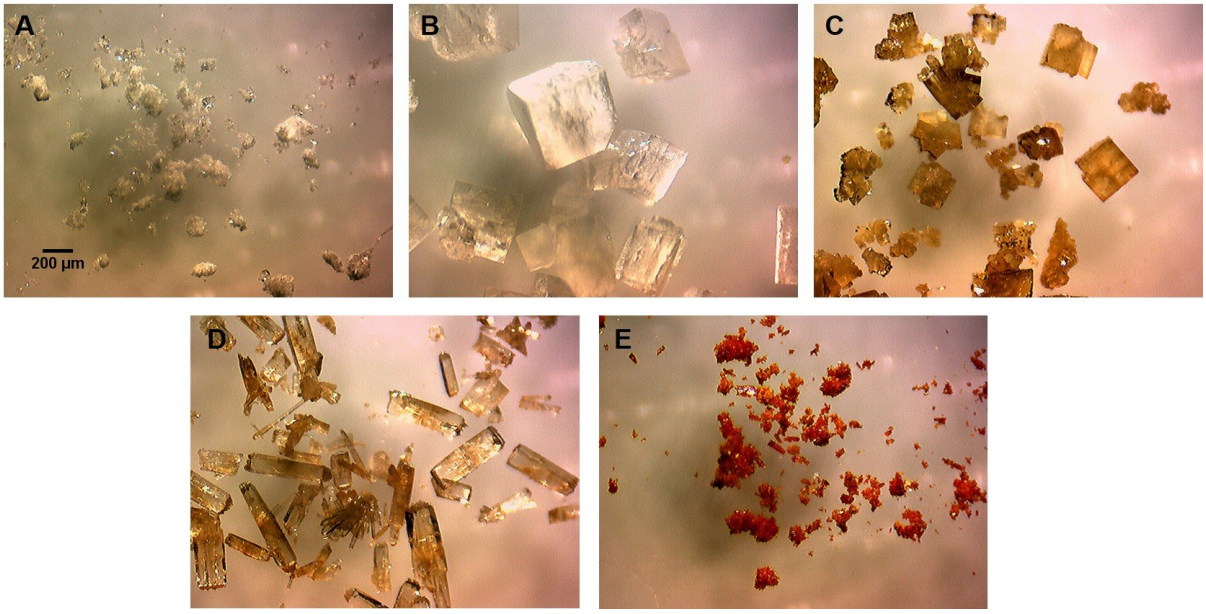

Figure 1. Microscope image of DMOF-1 (A), Br-DMOF-1 (B), NO_2-DMOF-1 (C), NH_2-DMOF-1 (D) and Azo-DMOF-1 (E) synthesized in this study (the scalebar is the same for all panels)

The product crystallinity was assessed using powder X-ray diffraction (PXRD). As can be seen in **Figure *2*** (A), all the synthesized materials are highly crystalline with the PXRD diffraction patterns of the functionalized DMOF-1s closely matching that of the non-functionalized DMOF-1, with a few notable differences. Firstly, the intensity of the first two peaks of Br-DMOF-1 are identical, which might be caused by crystals that crystallize in an orthorhombic space group with a rhomboidal pore shape compared with the distorted pore shape from its parent structure [7, 8]. There is also a slight difference observed in the PXRD diffraction pattern of the Azo-DMOF-1 at lower angles where the peak slightly shifts to a lower value. This might be caused by the accommodation process of the bulky structure from the azobenzene ligand [9]. As previously suggested, the presence of the benzene ring from the azobenzene functionality might slightly alter the DMOF-1 parent framework to more closely resemble the PXRD pattern of benzene-loaded DMOF-1 [1].

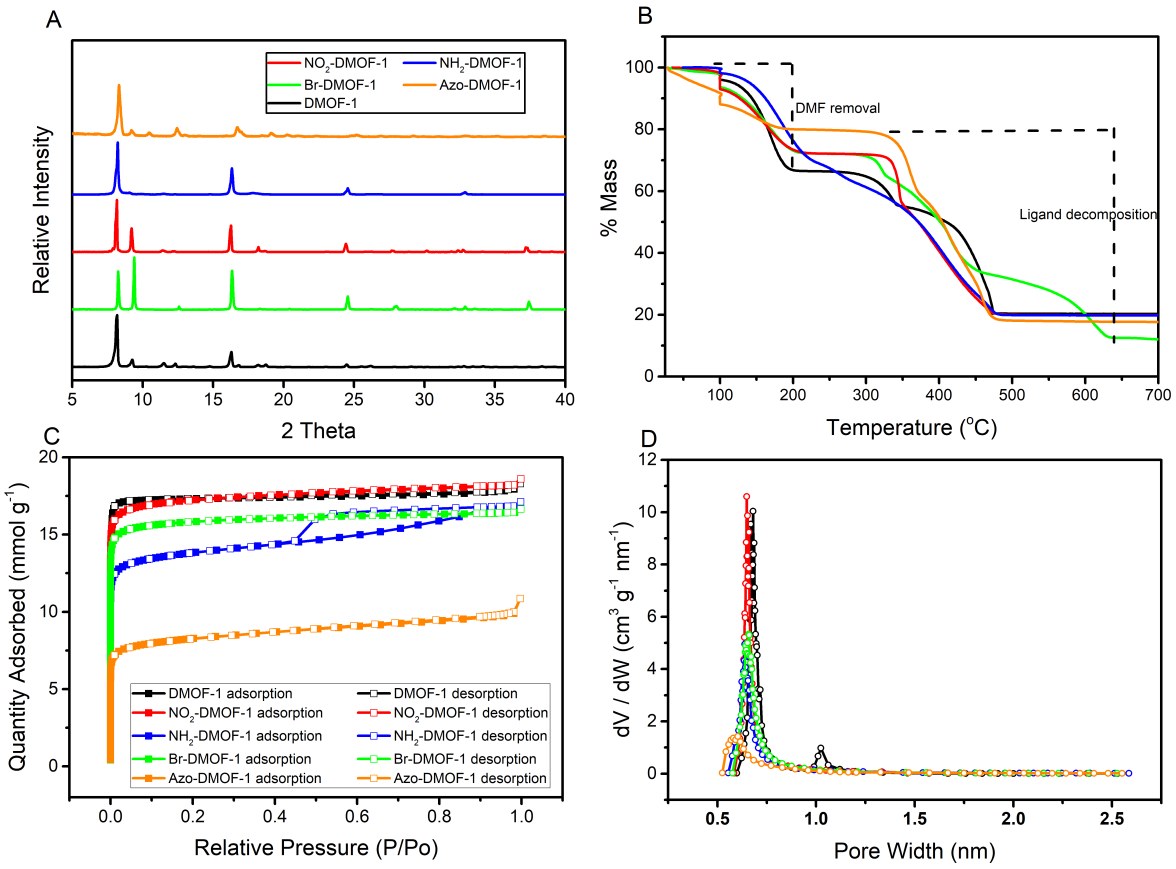

Figure 2. PXRD diffraction pattern (A), TGA analysis (B), N2 sorption at 77 K (C) and pore width distribution (D) of functionalized DMOF-1s synthesized in this study

The thermal stability of the materials was evaluated by heating in air in a thermogravimetric analyser, with the combined results presented in **Figure *2*** (B). Regardless of the DMOF-1 functionalisation, there are three different stages of mass loss. The first region likely results from the removal of DMF from the framework as DMF was the solvent used to synthesize the materials. The second and third step could then be ascribed to the two-step structural decomposition of the framework, since the MOFs were built from two different ligands which may decompose at distinctly different temperatures. However, a different behaviour was found in NH_2-DMOF-1. It was found that almost no stable region could be observed between 200-300 ^oC as observed with the rest of the MOFs. Rather, the mass was observed to continuously decrease within this range. As will be explained later, this behaviour might be caused by structural imperfection exhibited by the NH_2-DMOF-1 that might also impact its thermal stability behaviour.

The porosity of all functionalized DMOF-1 was analyzed via N_2 sorption isotherm collected at 77 K, and the results are presented in **Figure *2*** (C). Almost all the DMOF-1s synthesized in this study exhibit type-1 adsorption isotherms indicating the microporous structure of the functionalized DMOFs. However, a hysteresis does exist for NH_2-DMOF-1 which suggests the

presence of a mesoporous region. This finding then confirms a recent study showing the hysteresis obtained in NH_2-DMOF-1 which might be caused by the presence of 1D $Zn_2(H_2O)_2(NH_2\text{-BDC})$ and amorphous NH_2-DMOF-1 structure during the formation of perfect crystalline NH_2-DMOF-1 [10]. Their presence then contributes in building linker defects and a more flexible structure in the final DMOF-1 resulting in a mesoporous structure.

Table 1. Surface properties of functionalized DMOF-1s

MOF	BET Surface Area ($m^2\,g^{-1}$)	Max Pore Volume ($cm^3\,g^{-1}$)	Median pore width (nm)
DMOF-1	1161	0.601	0.68
NO_2-DMOF-1	1175	0.596	0.66
NH_2-DMOF-1	961.3	0.478	0.65
Br-DMOF-1	1074	0.548	0.66
Azo-DMOF-1	579.8	0.285	0.64

Table *1* then presents the BET surface area, maximum pore volume and median pore width of the MOFs used in this study. As can be seen, functionalizing DMOF-1 framework with NO_2 and Br does not then seem to negatively impact its surface property as they have a comparable value with the parent framework. Meanwhile lower surface area and pore volume exhibited by the NH_2-DMOF-1 compared with both NO_2-DMOF-1 and Br-DMOF-1 might be explained by the presence of structural imperfection as shown above in the hysteresis explanation in its N_2 sorption. In case of Azo-DMOF-1, the lowest surface area and pore volume is likely be caused by the bulkier structure of azobenzene functionality than for the other functional groups. In contrast, all the functionalized DMOF-1s had lower pore width in the range of 0.63-0.68 nm compared with its parent DMOF-1 which was found around 0.69 nm. The slight reduction of pore width could then be explained by the presence of various protruding functional groups inside the frameworks.

A further evaluation was then carried out to study the performance of various functionalized DMOF-1s for post-combustion CO_2 capture application since the polar functional groups could improve the CO_2 adsorption and separation property in MOFs [11]. This study was then carried out first by measuring the CO_2 uptake capacity of all the MOFs both at 273 and 298 K with the results presented in **Figure *3*** (A) and (B), respectively. First, as can be seen, the CO_2 uptake of DMOF-1 was found to be around 4.2 and 1.6 mmol g^{-1} at 273 and 298 K. These values are

also comparable with other findings reported on DMOF-1 [12]. Once functionalized ligands were used in DMOF-1, varieties were observed regarding this value. The CO_2 adsorption capacity in Br-DMOF-1 was observed to be around 4.6 and 1.9 mmol g^{-1} at 273 and 298 K, respectively. Meanwhile an increasing trend could be observed both in NH_2-DMOF-1 and NO_2-DMOF-1. In NH_2-DMOF-1, this value could be increased to be around 5.5 and 2.5 mmol g^{-1} at 273 and 298 K, respectively. Meanwhile for NO_2-DMOF-1, the CO_2 adsorption capacity was found to be around 5.8 and 2.5 mmol g^{-1} at 273 and 298 K, respectively. In contrast, a decreasing trend could be observed in Azo-DMOF-1 as its CO_2 uptake capacity was found to be around 2.8 and 1.4 mmol g^{-1} at 273 and 298 K, respectively.

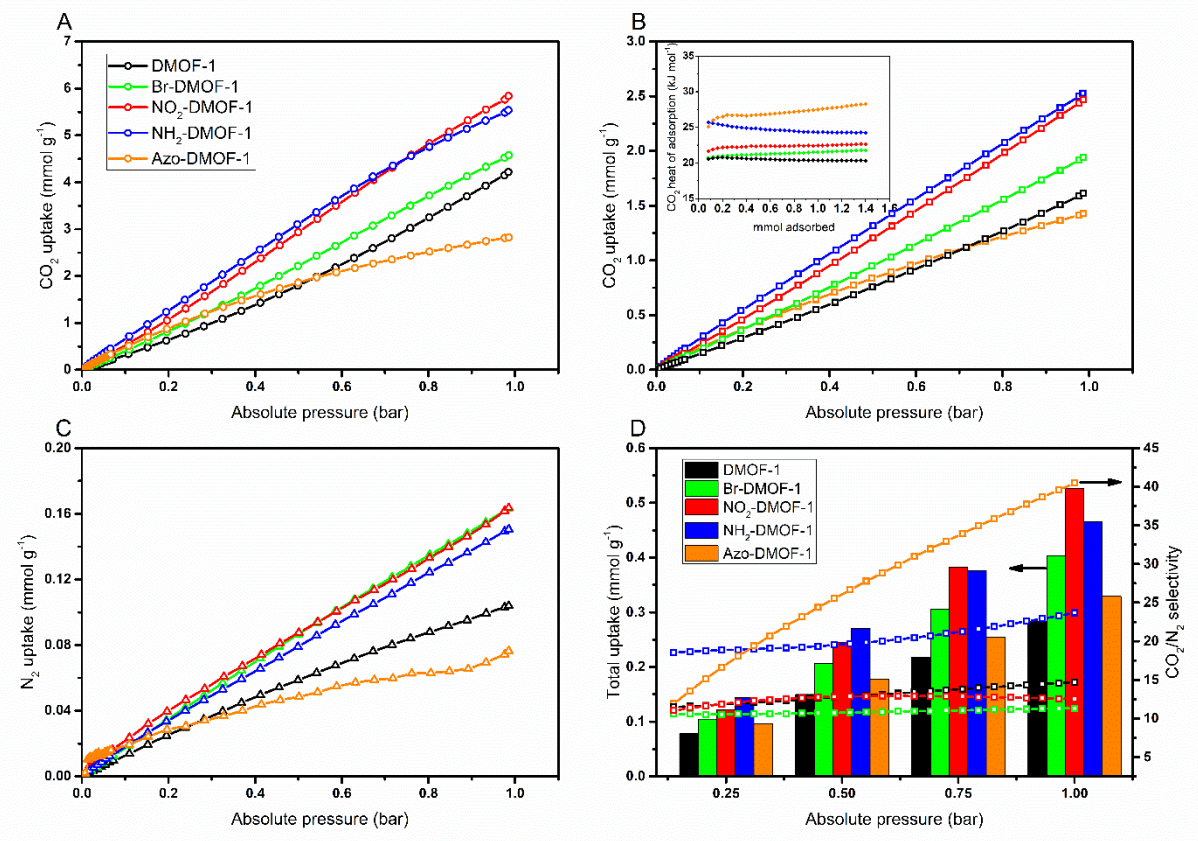

Figure 3. CO_2 adsorption at 273 K (A) and 298 K (B), N_2 uptake at 298 K (C) and CO_2/N_2 (15:85) IAST selectivity at 298 K (D) of the functionalized DMOF-1s. Inset of Figure 3 (B): CO_2 heat of adsorption of functionalized DMOF-1s

From these results, it could be observed that although both NH_2-DMOF-1 and NO_2-DMOF-1 have lower surface area compared with the DMOF-1, both amino and nitro group could be considered as polar groups that could enhance the interaction between the MOF framework and CO_2 resulting in overall increase in CO_2 uptake [11, 13]. This is also corroborated by the CO2 heat of adsorption of both MOFs which are found to be around 23 and 25 kJ mol-1 for NO2-DMOF-1 and NH2-DMOF-1, respectively, as can be seen in the inset of Figure 3 (B). These values are higher compared with the parent MOF which was found to be around 20 kJ

mol-1 which is comparable with other findings [5, 14, 15]. The higher CO2 heat of adsorption value exhibited by both NO2-DMOF-1 and NH2-DMOF-1 then indicates more favourable interaction between CO_2 and both frameworks rather than DMOF-1. Meanwhile a decreasing trend in CO_2 uptake in Azo-DMOF-1 is expected since it has the lowest surface area compared with the rest of the MOFs used in this study. This then results in the overall reduction of CO_2 uptake capacity of Azo-DMOF-1. Interestingly, the decreasing trend of CO_2 uptake in Azo-DMOF-1 was not accompanied by the decrease of CO_2 heat of adsorption which was found to be around 28 kJ mol^{-1} at high coverage. This value is even higher than both NH_2-DMOF-1 and NO_2-DMOF-1 and comparable with other MOFs designed for CO_2 capture [16-19]. This then indicates a more favourable interaction between CO_2 and the framework which could be caused by the Lewis acid-base interaction between the CO_2 and azobenzene functionality [20].

Ideal Adsorbed Solution Theory (IAST) was then employed to further evaluate the CO_2/N_2 separation performance [21]. A scenario of 15:85 mixture of CO_2:N_2 was used for the calculation in order to simulate the flue gas composition from a coal-fired power plant [22]. The result is then presented in **Figure *3*** (D). First, it could be seen that the CO_2/N_2 selectivity of DMOF-1 was found to be around 15 with a total uptake to be around 0.28 mmol g^{-1}. This value is also comparable with previous findings when studying DMOF-1 for CO_2/N_2 separation [14, 15]. For the functionalized DMOF-1s, it could be seen that their uptake capacity could be increased compared with the parent MOF. This might be explained by the higher CO_2 uptake capacity and heat of adsorption of the functionalized DMOF-1 which could increase both the capacity and affinity between the functionalized DMOF-1 and the CO_2. However, only NH_2-DMOF-1 and Azo-DMOF-1 showed a higher CO_2/N_2 selectivity value compared with DMOF-1 while a slight decrease was observed both for NO_2-DMOF-1 and Br-DMOF-1. The CO_2/N_2 selectivity for Azo-DMOF-1 and NH_2-DMOF-1 was found to be around 40 and 25, respectively. This selectivity value is comparable, or higher in case of Azo-DMOF-1, with other MOF designed for post-combustion CO_2 capture such as PCN-88 [23], Ni-AG15 [24] and Ni-MOF-1 [25].

This phenomenon could then be explained two ways. First, higher CO_2 heat of adsorption observed in functionalized DMOF-1 might help to increase its affinity with CO_2 resulting in higher selectivity. However, this could not fully explain the phenomenon as higher selectivity was not observed in all functionalized DMOF-1s and the Azo-DMOF-1 had higher selectivity compared with the NH_2-DMOF-1. Therefore, another mechanism might play a role which is more related with N_2 interaction with the framework. It could be seen in **Figure *3*** (C) that all the N_2 uptake curves in Azo-DMOF-1 were different to the rest of the functionalized DMOF-1s. The trend was observed to be plateauing rather than linearly increasing as observed with

the rest. This might then indicate that the affinity of N_2 with Azo-DMOF-1 is weaker than with the NH_2-DMOF-1. A decrease in N_2 affinity towards porous framework have also been reported previously in organic-based porous materials [26]. With higher N_2 concentration than CO_2 in the feed composition, this also means that the competitive adsorption in Azo-DMOF-1 might be less demanding than in the NH_2-DMOF-1 since the framework of the former is more N_2-phobic compared with the later. As a result, the CO_2 would have higher tendency to adsorb on the surface of Azo-DMOF-1 and thus higher selectivity was obtained. This phenomenon was also previously observed with azobenzene-based porous materials where higher CO_2/N_2 was observed because of the lower affinity between the framework and N_2 [26]. This then highlights the benefit of having azobenzene functionality in DMOF-1 apart from the potential to use UV light as a sustainable source for material regeneration after the CO_2 capture [9, 27].

In conclusion, this study has shown that functionalizing DMOF-1s with various functional groups within its framework is beneficial to increase their affinity towards CO_2 as indicated by higher CO_2 heat of adsorption and resulting in higher CO_2 uptake capacity. However, in case where competitive adsorption occurs between CO_2 and N_2, functionalizing the DMOF-1 with azobenzene group seems to have the best impact since the steric effect of the azobenzene could also impart an additional N_2-phobic environment in the framework resulting in higher CO_2/N_2 selectivity. However, in case where CO_2 concentration is higher and less adsorption competition occurs, this steric effect might not be so beneficial since it also hinders the CO_2 adsorption on the surface resulting in slightly lower selectivity and lower CO_2 uptake capacity.

Acknowledgments

N.P acknowledges the PhD scholarship funding from the Department of Chemical Engineering, Imperial College London. M. X acknowledges the UROP funding from Department of Chemical Engineering, Imperial College London.

Data Repository

Full resolution optical and SEM images and high-resolution copies of the figures used in this manuscript are available from the open repository: https://doi.org/10.5281/zenodo.3332915

References

[1] D.N. Dybtsev, H. Chun, K. Kim, Rigid and flexible: A highly porous metal-organic framework with unusual guest-dependent dynamic behavior, Angew. Chemie - Int. Ed. 43 (2004) 5033–5036. doi:10.1002/anie.200460712.

[2] S. Henke, A. Schneemann, A. Wütscher, R.A. Fischer, Directing the breathing behavior of pillared-layered metal-organic frameworks via a systematic library of

functionalized linkers bearing flexible substituents, J. Am. Chem. Soc. 134 (2012) 9464–9474. doi:10.1021/ja302991b.

[3] S. Henke, R. Schmid, J.-D. Grunwaldt, R.A. Fischer, Flexibility and Sorption Selectivity in Rigid Metal-Organic Frameworks: The Impact of Ether-Functionalised Linkers, Chem. - A Eur. J. 16 (2010) 14296–14306. doi:10.1002/chem.201002341.

[4] Z. Wang, K.K. Tanabe, S.M. Cohen, Tuning Hydrogen Sorption Properties of Metal-Organic Frameworks by Postsynthetic Covalent Modification, Chem. - A Eur. J. 16 (2010) 212–217. doi:10.1002/chem.200902158.

[5] S. Chaemchuen, K. Zhou, N.A. Kabir, Y. Chen, X. Ke, G. Van Tendeloo, F. Verpoort, Tuning metal sites of DABCO MOF for gas purification at ambient conditions, Microporous Mesoporous Mater. 201 (2015) 277–285. doi:10.1016/j.micromeso.2014.09.038.

[6] H. Kim, D.G. Samsonenko, S. Das, G.-H. Kim, H.-S. Lee, D.N. Dybtsev, E.A. Berdonosova, K. Kim, Methane Sorption and Structural Characterization of the Sorption Sites in Zn 2 (bdc) 2 (dabco) by Single Crystal X-ray Crystallography, Chem. - An Asian J. 4 (2009) 886–891. doi:10.1002/asia.200900020.

[7] L.K. Cadman, J.K. Bristow, N.E. Stubbs, D. Tiana, M.F. Mahon, A. Walsh, A.D. Burrows, Compositional control of pore geometry in multivariate metal–organic frameworks: an experimental and computational study, Dalt. Trans. 45 (2016) 4316–4326. doi:10.1039/C5DT04045K.

[8] K. Uemura, Y. Yamasaki, F. Onishi, H. Kita, M. Ebihara, Two-Step Adsorption on Jungle-Gym-Type Porous Coordination Polymers: Dependence on Hydrogen-Bonding Capability of Adsorbates, Ligand-Substituent Effect, and Temperature, Inorg. Chem. 49 (2010) 10133–10143. doi:10.1021/ic101517t.

[9] N. Prasetya, B.P. Ladewig, New Azo-DMOF-1 MOF as a Photoresponsive Low-Energy CO 2 Adsorbent and Its Exceptional CO 2 /N 2 Separation Performance in Mixed Matrix Membranes, ACS Appl. Mater. Interfaces. 10 (2018) 34291–34301. doi:10.1021/acsami.8b12261.

[10] D.T. Mcgrath, V.A. Downing, M.J. Katz, Investigating the crystal engineering of the pillared paddlewheel metal-organic framework Zn 2 IJNH 2 BDC) 2 DABCO †, (2018). doi:10.1039/c8ce00848e.

[11] G.E. Cmarik, M. Kim, S.M. Cohen, K.S. Walton, Tuning the Adsorption Properties of UiO-66 via Ligand Functionalization, Langmuir. 28 (2012) 15606–15613. doi:10.1021/la3035352.

[12] Y. Zhao, H. Wu, T.J. Emge, Q. Gong, N. Nijem, Y.J. Chabal, L. Kong, D.C. Langreth, H. Liu, H. Zeng, J. Li, Enhancing gas adsorption and separation capacity through ligand functionalization of microporous metal-organic framework structures, Chem. - A Eur. J. 17 (2011) 5101–5109. doi:10.1002/chem.201002818.

[13] S. Biswas, P. Van Der Voort, A general strategy for the synthesis of functionalised UiO-66 frameworks: Characterisation, stability and CO2 adsorption properties, Eur. J. Inorg. Chem. (2013) 2154–2160. doi:10.1002/ejic.201201228.

[14] Z. Liang, M. Marshall, A.L. Chaffee, CO2 adsorption, selectivity and water tolerance of pillared-layer metal organic frameworks, Microporous Mesoporous Mater. 132 (2010) 305–310. doi:10.1016/j.micromeso.2009.11.026.

[15] P. Mishra, S. Edubilli, B. Mandal, S. Gumma, Adsorption of CO2, CO, CH4 and N2 on DABCO based metal organic frameworks, Microporous Mesoporous Mater. 169 (2013) 75–80. doi:10.1016/j.micromeso.2012.10.025.

[16] C. Lv, W. Li, Y. Zhou, J. Li, Z. Lin, A new porous Ca(II)-organic framework with acylamide decorated pores for highly efficient CO2 capture, Inorg. Chem. Commun. 99 (2019) 40–43. doi:10.1016/j.inoche.2018.11.008.

[17] C.-L. Gao, J.-Y. Nie, Preferential CO2 adsorption and theoretical simulation of a Cu(II)-based metal-organic framework with open-metal sites and basic groups, Inorg. Chem. Commun. 102 (2019) 199–202. doi:10.1016/J.INOCHE.2019.02.029.

[18] M.-Y. Sun, D.-M. Chen, A microporous metal-organic framework with unusual 2D → 3D polycatenation for selective sorption of CO2 over CH4 at room temperature, Inorg. Chem. Commun. 89 (2018) 18–21. doi:10.1016/J.INOCHE.2018.01.011.

[19] S. Xiang, Y. He, Z. Zhang, H. Wu, W. Zhou, R. Krishna, B. Chen, Microporous metal-organic framework with potential for carbon dioxide capture at ambient conditions, Nat. Commun. 3 (2012) 954. doi:10.1038/ncomms1956.

[20] P. Arab, E. Parrish, T. İslamoğlu, H.M. El-Kaderi, Synthesis and evaluation of porous azo-linked polymers for carbon dioxide capture and separation, J. Mater. Chem. A. 3 (2015) 20586–20594. doi:10.1039/C5TA04308E.

[21] S. Lee, J.H. Lee, J. Kim, User-friendly graphical user interface software for ideal adsorbed solution theory calculations, Korean J. Chem. Eng. 35 (2018) 214–221. doi:10.1007/s11814-017-0269-9.

[22] M. Oschatz, M. Antonietti, A search for selectivity to enable CO2 capture with porous adsorbents, Energy Environ. Sci. 11 (2018) 57–70. doi:10.1039/C7EE02110K.

[23] J.-R. Li, J. Yu, W. Lu, L.-B. Sun, J. Sculley, P.B. Balbuena, H.-C. Zhou, Porous materials with pre-designed single-molecule traps for CO2 selective adsorption, Nat. Commun. 4 (2013) 1538. doi:10.1038/ncomms2552.

[24] L. Asgharnejad, A. Abbasi, A. Shakeri, Ni-based metal-organic framework/GO nanocomposites as selective adsorbent for CO2 over N2, Microporous Mesoporous Mater. 262 (2018) 227–234. doi:10.1016/J.MICROMESO.2017.11.038.

[25] L. Wang, R. Zou, W. Guo, S. Gao, W. Meng, J. Yang, X. Chen, R. Zou, A new microporous metal-organic framework with a novel trinuclear nickel cluster for selective CO2 adsorption, Inorg. Chem. Commun. 104 (2019) 78–82. doi:10.1016/J.INOCHE.2019.03.029.

[26] H.A. Patel, S. Hyun Je, J. Park, D.P. Chen, Y. Jung, C.T. Yavuz, A. Coskun, Unprecedented high-temperature CO2 selectivity in N2-phobic nanoporous covalent organic polymers, Nat. Commun. 4 (2013) 1357. doi:10.1038/ncomms2359.

[27] R. Lyndon, K. Konstas, B.P. Ladewig, P.D. Southon, P.C.J. Kepert, M.R. Hill, Dynamic Photo-Switching in Metal-Organic Frameworks as a Route to Low-Energy Carbon Dioxide Capture and Release, Angew. Chemie Int. Ed. 52 (2013) 3695–3698. doi:10.1002/anie.201206359.

Supplementary Information

Systematic screening of DMOF-1 with NH_2, NO_2, Br and azobenzene functionalities for elucidation of carbon dioxide and nitrogen separation properties

Mingrou Xie, Nicholaus Prasetya and Bradley P. Ladewig

Synthesis Method of functionalised DMOF-1s

For each DMOF-1, zinc nitrate ($Zn(NO_3)_2$), functionalised terephthalic acid ($C_6H_4(COOH)_2$, bdc), and 1,4-diazabicyclo[2.2.2]octane ($N_2(C_2H_4)_3$, DABCO) were mixed in a 1:1:0.5 mmol ratio in 20ml of dimethylformamide ($(CH_3)_2NCH$, DMF). The mixture was ultrasonicated for 10mins in a water bath to dissolve the reagents. Precursor solution colours are noted in Table S1.

Table S1. DMOF-1 solution and crystal colours

Functionalised DMOF-1	Precursor Solution Colour	Post-synthesis Solution Colour	Post-synthesis Crystal Colour
DMOF-1	Cloudy white	Colourless	Colourless
Azo-DMOF-1	Clear and bright orange	Brown	Orange
NO_2-DMOF-1	Clear and light orange	Brown	Brown
NH_2-DMOF-1	Clear and light yellow	Brown	Brown
Br-DMOF-1	Clear and colourless	Colourless	Colourless

NO_2-DMOF-1, Azo-DMOF-1 and DMOF-1 precursor solutions were heated at 120°C for 48h. Br-DMOF-1 and NH_2-DMOF-1 precursor solutions were heated at 120°C for 24h, producing crystals in solution as described in Table S1.

Characterization of functionalised DMOF-1s

Optical and electron microscopy

Microscope images of all the materials were taken by using a MOTIC microscope image processing software. Meanwhile, for the scanning electron microscopy (SEM) images, all the micrographs of the gold-sputtered samples were taken by using FEGSEM Sigma 300 instrument. The accelerating voltage was set at 5 kV.

Powder X-Ray diffraction (PXRD)

PXRD diffraction pattern of all the materials were collected using PANanalytical instrument under ambient condition. During the measurement, the samples were spun and the voltage and current of the instrument were set at 40 kV and 20 mA, respectively. Diffraction patterns were collected between 5 and 40 theta with 0.008° sample step.

Thermal analysis

Thermal analysis of all the materials were collected using Netzsch TG 20 F1 Libra instrument. About 10 mg of samples was used during the measurement. The heating rate was set at 5 K min^{-1} under air atmosphere flowing at 20 ml min^{-1}

N_2 and CO_2 sorption

Both N_2 and CO_2 adsorption data were taken by using 3Flex Micromeritics instrument. The samples were activated at 120°C under vacuum overnight before the measurement took place. N_2 sorption isotherms were collected at 77 K. Meanwhile CO_2 adsorption were taken at both 273 and 298 K. Additional N_2 uptake was also carried out at 298 K to analyse the CO_2/N_2 separation performance of the materials.

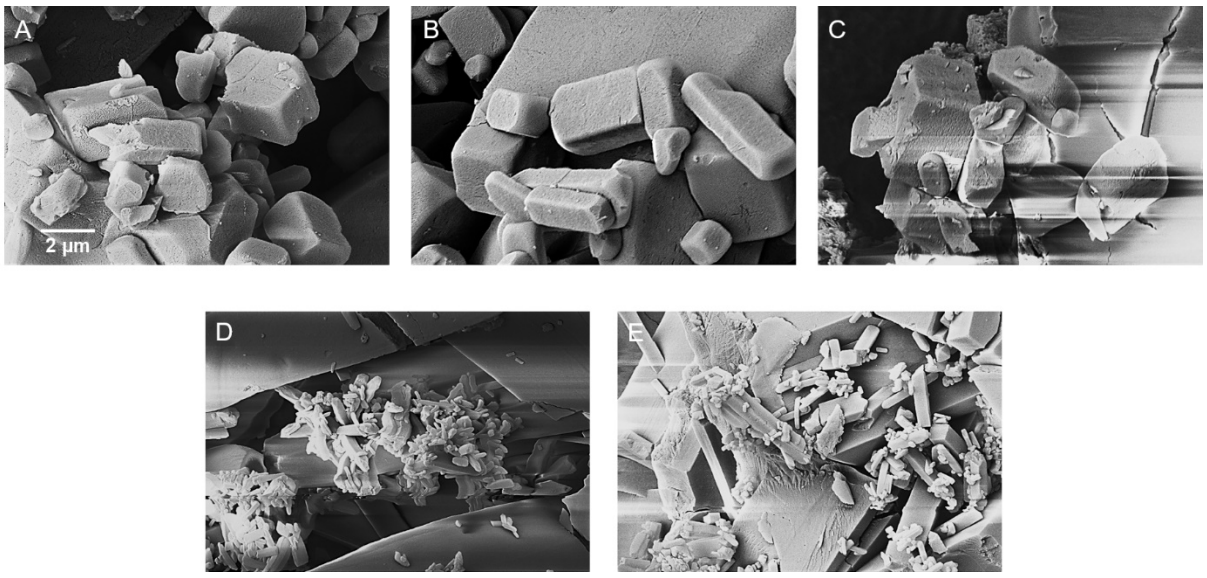

Figure S 1.Additional SEM images of DMOF-1 (A), Br-DMOF-1 (B), NO_2-DMOF-1 (C), NH_2-DMOF-1 (D) and Azo-DMOF-1 (E)

The ^{1}H-NMR spectra of the digested DMOF-1s could be seen in Figure S2-S6. It should be noted that the peak at around 4.8 ppm comes from water and for some spectrum there are also traces of DMF (as this was used the solvent) as observed in peaks coming at around 2.5 ppm, 2.8 ppm and 8 ppm.

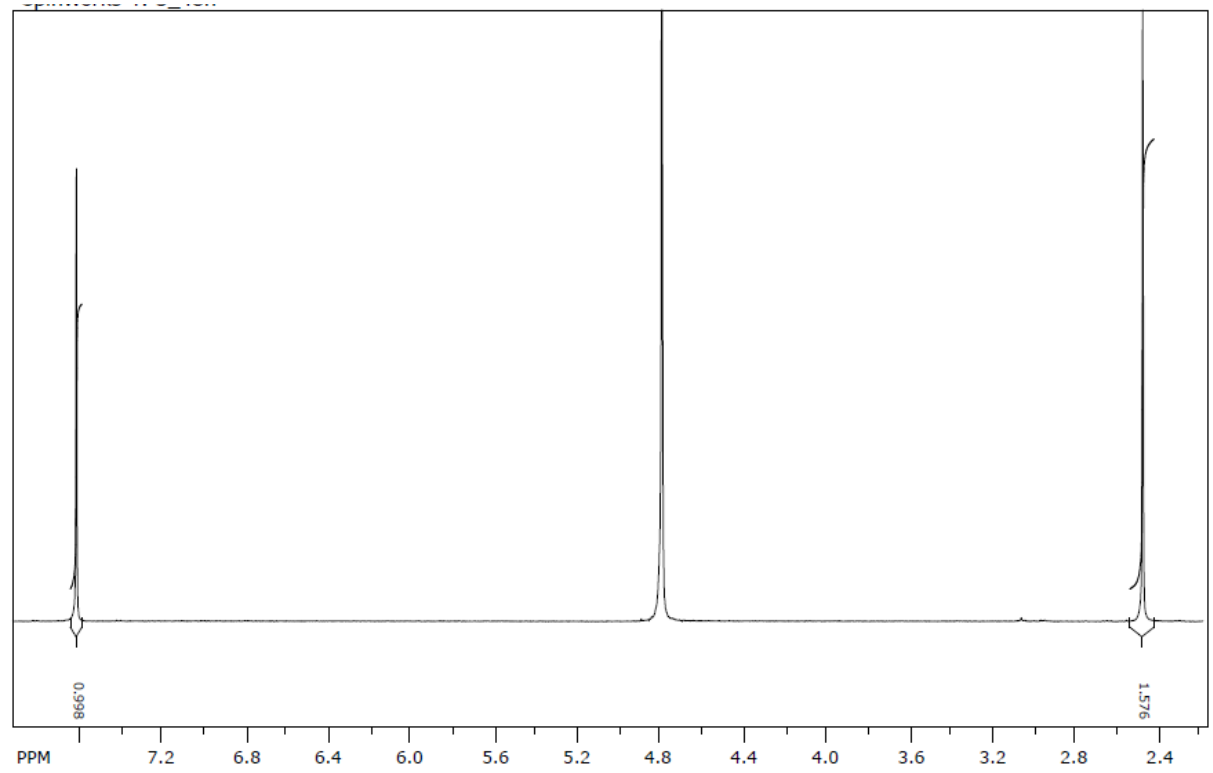

Figure S 2. ^{1}H-NMR spectrum of digested DMOF-1

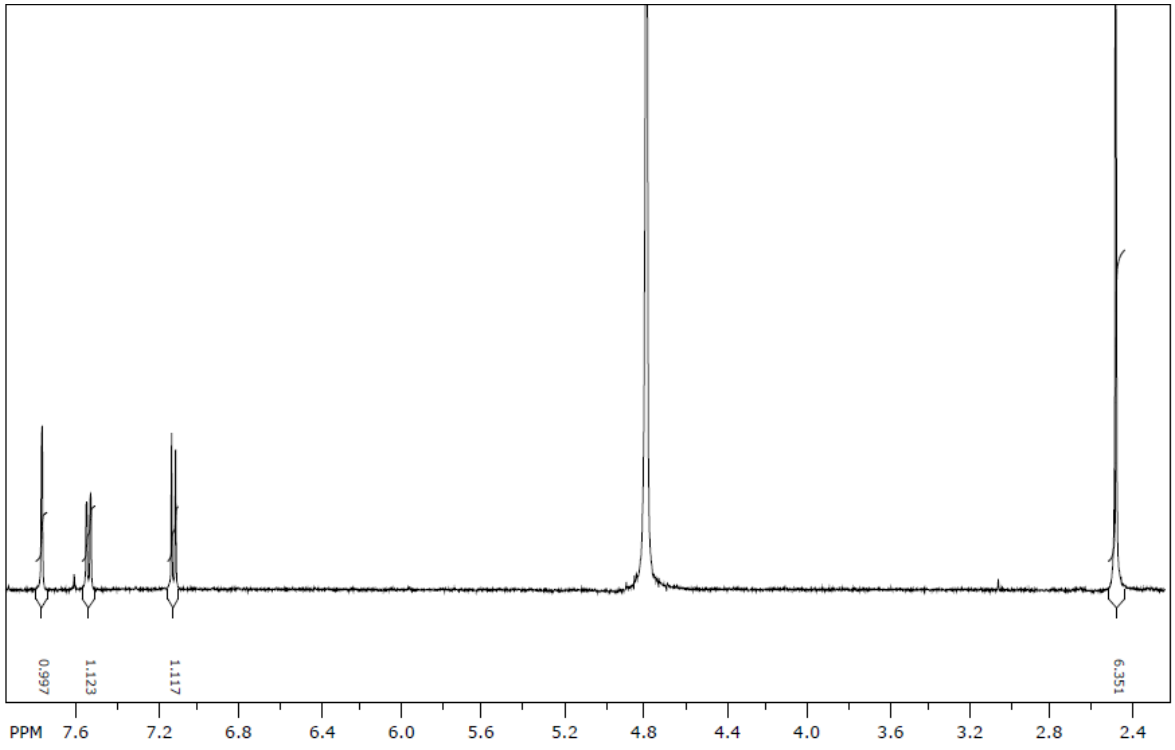

Figure S 3. ^{1}H-NMR spectrum of digested Br-DMOF-1

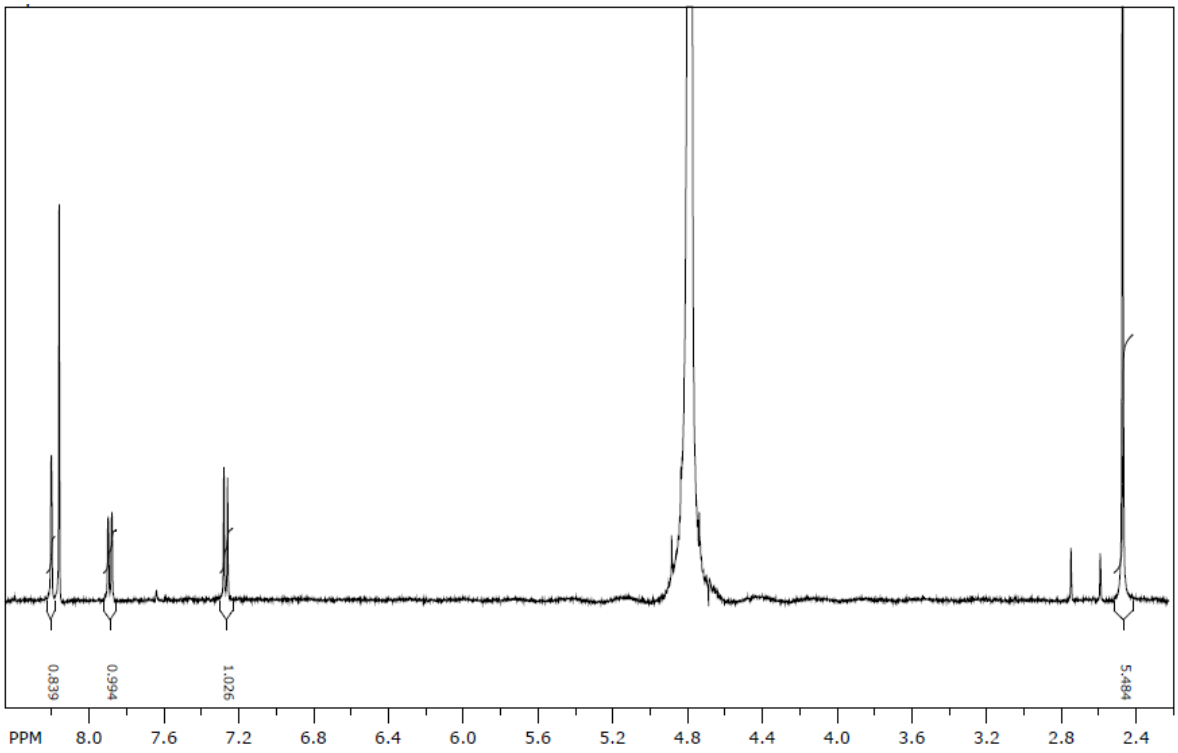

Figure S 4. ^{1}H-NMR spectrum of digested NO_2-DMOF-1

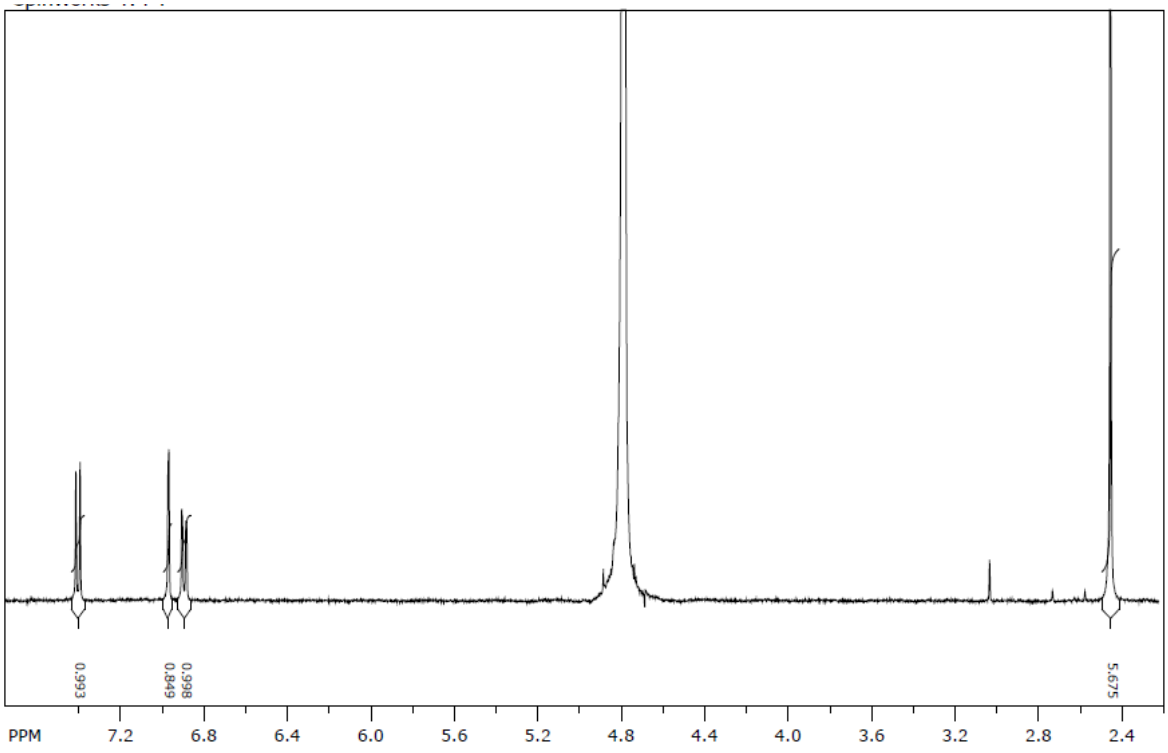

Figure S 5. ^{1}H-NMR spectrum of digested NH_2-DMOF-1

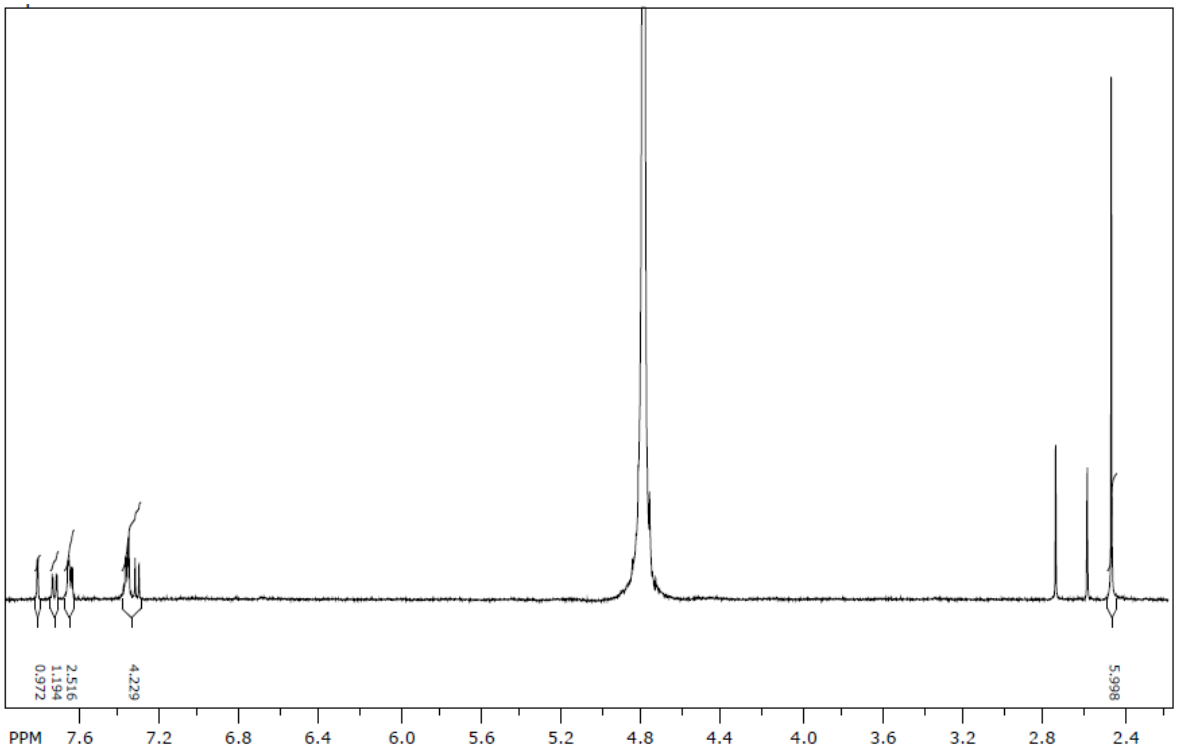

Figure S 6. ^{1}H-NMR spectrum of digested Azo-DMOF-1